

**Silvio Francisco Brunatto**

brunatto@ufpr.br  
Federal Univ. of Paraná – UFPR  
Department of Mechanical Engineering  
81531-990 Curitiba, PR, Brazil

**Aloísio Nelmo Klein**

Federal Univ. of Santa Catarina – UFSC  
Department of Mechanical Engineering  
88000-000 Florianópolis, SC, Brazil

**Joel Louis Rene Muzart**

Federal Univ. of Santa Catarina – UFSC  
Department of Mechanical Engineering  
88000-000 Florianópolis, SC, Brazil  
In memoriam

# Hollow Cathode Discharge: Application of a Deposition Treatment in the Iron Sintering

*The influence of a previous deposition treatment on the final amount of alloying elements (Cr and Ni) deposited and diffused into the surface of iron parts sintered in hollow cathode discharge (HCD) was studied. Cylindrical pure iron pressed samples, being a central cathode, were placed concentrically in the interior of an AISI 310 steel machine-made outer cathode, resulting in a 6 mm inter-cathode radial spacing. The study was divided in two steps: a) deposition treatment with the outer cathode acting as target and the iron sample acting as substrate (1123K -850 °C- and 60 minutes deposition temperature and time, respectively); and b) deposition treatment plus HCD sintering (1423K -1150 °C- and 60 minutes sintering temperature and time, respectively). The electrical discharge was generated using a pulsed voltage power source. The results indicate the presence of 6.5 at.% Cr and 6.9 at.% Ni on the samples surface. The concentration profiles were mathematically treated to quantify the actual amounts of Cr and Ni deposited on and diffused into the samples, and the integration of the fitted equations yielded the calculated areas of 133 ( $\mu\text{m} \times \text{at.}\% \text{Cr}$ ) and 105 ( $\mu\text{m} \times \text{at.}\% \text{Ni}$ ), respectively.*

**Keywords:** hollow cathode discharge, plasma sintering, alloying elements deposition, sputtering

## Introduction

The use of plasma-assisted techniques in the field of materials processing has increased steadily in recent years. The possibility of altering the material's surface characteristics by exposing it to plasma species has led to the development of new techniques and processes.

Sintering techniques using electrical discharges can be divided into three major groups: a) Direct Current Abnormal Glow Discharge Sintering (Muzart et al., 1997); b) Microwave or Radio-Frequency Glow Discharge Sintering (Bengisu and Inal, 1994; Tandian and Pfender, 1997; Su and Jhonson, 1996); and c) Spark-Plasma Activated Sintering (Onagawa et al., 1996; Jones et al., 1994).

Direct Current Abnormal Glow Discharge (linear discharge) is preferentially recommended for the processing of metallic materials, since metals normally present high electrical conductivity (Muzart et al., 1997). In this process, the pressed sample to be sintered is placed inside the cathode, and sufficiently high temperatures can be reached to sinter metals by bombarding the cathode with plasma species.

Recently, sintering of metallic components using an abnormal glow discharge containing hydrogen and argon has been described (Batista et al., 1998). The abnormal glow discharge is characterized by full covering of the cathode by the glow region (Chapman, 1980), supplying a uniform treatment. The principle of heating is based on the ion and fast neutrals bombardment of the sample. A negatively biased voltage was applied to the sample, which worked as the cathode of the abnormal glow discharge, generating an electric field in the cathode sheath, where ions are strongly accelerated. Collisions between ions and argon atoms or hydrogen molecules of the gas discharge in the cathode sheath result in a flow of fast neutrals toward the cathode (Chapman, 1980). The bombardment of ions and fast neutrals heat the sample.

Direct Current Hollow Cathode Discharge in abnormal regime (exponential discharge) is a variant of the first group of discharge techniques, whose cathode geometry produces a discharge different from the linear glow discharge. The hollow cathode effect was first described by Paschen in 1916 (after v. Engel, 1994). This effect

occurs in cathodes presenting cavities, hollows or even parallel faces, when the discharge fills the cavity under given conditions governed by the "axp" product (a = inter-cathode spacing and p = gas pressure).

The modified linear abnormal glow discharge, using the hollow cathode configuration, also results in the bombardment of the cathode by ions and fast neutrals, consequently causing its heating. Using the hollow cathode geometry, the ionization rate is higher than that of the linear abnormal glow discharge. As a result, an increased heating efficiency is obtained in the same proportion as compared to the linear discharge. In addition, the high ionisation rate not only increases the heating efficiency but also enhances the sputtering (Chapman, 1980; Benda et al., 1997; Koch et al., 1991). So, an efficient process for sintering pressed sample can be expected leading to the simultaneous sintering of it and modification of the chemical composition of its surface, as a consequence of the sputtering.

The hollow cathode effect causes an increase of the current density (and hence the cathode temperature) even at low pressures (normally under 9 torr), in response to an exponential multiplication of electrons produced by ionization in cathode sheaths (Kolobov and Tsendin, 1995). This effect is accomplished by increasing both the secondary electron emission rate and through the sputtering mechanism (Benda et al., 1997; Koch et al., 1991). Due to the negative potential of cathode sheaths, the secondary electron beams emitted from each cathode surface are repulsed toward the region of negative glow (in an oscillatory motion between the cathode walls), keeping the electrons energized upon discharge (Fig. 1). Basically, exponential hollow cathode discharges are differentiated from linear glow discharges by high-energy electrons arrested between the cathode walls (Kolobov and Tsendin, 1995; Hashiguchi and Hasikuni, 1987).

In practice, considering the various possible geometries and arrangements, the hollow cathode effect occurs with "axp" products ranging from 0.375 to 3.75 cm.torr (Koch et al., 1991). For monoatomic gases, this range may expand up to 10 cm.torr (Schaefer et al., 1984). Studies using annular discharges have been conducted for intercathode radial spacing varying from 0.3 to 3.0 cm (Terakado et al., 1996; Timanyuk and Tkachenko, 1989).

Based on the characteristics of the hollow cathode (annular) discharge, two alternatives proved viable: (a) sintering metallic samples placed in the central cathode, and (b) altering their chemical

surface composition using an outer hollow cathode with a different chemical composition (Brunatto et al., 2001).

In this paper, a D.C. pulsed hollow cathode discharge in an argon/hydrogen gas mixture was used to sinter unalloyed iron samples placed in the central cathode. The advantage of using a mixture of Ar + H<sub>2</sub> lies in the production of hydrogen atoms and a consequent reduction of the oxides present in the pressed pellets. The hollow cathode configuration, comprising an annular discharge (Timanyuk et al., 1989), consisted of a hollow cylinder part made of AISI 310 stainless steel (the external cathode) positioned concentrically in relation to the central cathode. In accordance with (Brunatto et al., 2005), the external cathode produced a plasma-confined geometry as well as a source of alloying elements, which were sputtered and deposited on the samples' surfaces by diffusion in the gas phase. Emphasis is given to the alternative procedure study of a previous deposition treatment in the sintering of iron samples in hollow cathode discharge. Results obtained for two different process conditions are confronted: a) hollow cathode discharge sintering without previous deposition treatment; and b) previous deposition treatment, with the outer cathode acting as target and the iron sample acting as substrate, following on the hollow cathode discharge sintering. The paper is divided in two parts. Special attention focuses in the first part on the variations of the discharge parameters under the different conditions studied here, where a preliminary hollow cathode discharge sintering study as a function of the pressure is also presented. The second part discusses the effects of previous deposition treatment and sintering time on the samples' surface characteristics. The sputtering-related aspects were analysed in terms of the concentration of alloying elements (Cr and Ni) deposited on the samples' surfaces and the formation of a layer containing these elements, and the morphology of the surfaces exposed to the plasma.

## Experimental Procedure

Figure 1 consists of an *in situ* view of the annular glow discharge. A weak luminosity corresponding to the linear discharge can be observed on the outside of the external cathode and an intense glow in the inter-cathode region, which results from the high ionization rate is attained in the hollow cathode configuration. The plasma-sintering chamber, comprising the anode, consisted of a stainless steel cylinder 350 mm in diameter and 380 mm in height. Detailed representation of the experimental apparatus is available in the earlier reports (Brunatto et al., 2001; 2005).

Samples 10 mm in diameter and 10 mm in high were placed on an AISI 1008 steel support (10 mm in diameter and 12 mm in high) that functions as the central cathode of the discharge. Samples of unalloyed iron were produced using Ancorsteel 1000C iron powder (99.75 wt% pure). A double action press with moving die body was used to press the samples that had a green density of  $7.0 \pm 0.1 \text{ g cm}^{-3}$ . The mass of the pressed samples was typically around 5.0 g. The external cathode was an AISI 310 (24.50% Cr, 16.20% Ni, 1.50% Mn, 1.50% Si, 0.03% C, balance in Fe, in atoms) stainless steel cylinder, located concentrically to the sample. The diameter of the external cathode was 22 mm corresponding to inter-cathode distances of 6 mm, respectively. The height of the external cylinder was 25 mm and the central cathode consisted of the support, the sample and a cylinder on the top, such that the central cathode total height was also 25 mm, so as to generate a uniform electric field and consequently a homogeneous discharge.

Prior to sintering, the system was pumped down by a two-stage mechanical pump until a residual pressure of less than 1.33 Pa (0.01 Torr) was reached. The gas mixture consisting of 80% argon (99.999% pure) and 20% hydrogen (99.998% pure) was adjusted using two datametrics mass flow controllers whose full scale value

was  $8.3 \times 10^{-6}$  standard  $\text{m}^3\text{s}^{-1}$  (500 sccm) and  $3.3 \times 10^{-6}$  standard  $\text{m}^3\text{s}^{-1}$  (200 sccm), respectively. The total gas flow was set to  $5 \times 10^{-6}$  standard  $\text{m}^3\text{s}^{-1}$  (300 sccm) in order to maintain a 'clean' atmosphere of the discharge. The pressure in the vacuum chamber was adjusted by manual valves and measured using an Edward capacitance manometer of  $1.33 \times 10^3$  Pa (10 Torr) full scale.

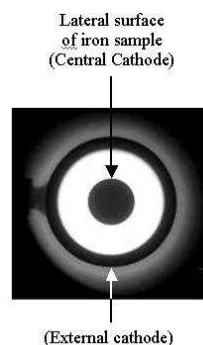


Figure 1. *In situ* view of the annular glow discharge.

For the first studied process condition, *id est* hollow cathode discharge sintering without previous deposition treatment, both cathodes were negatively biased at the same voltage, using a square form pulsed power supply of 3.6 kW. The applied voltage ( $V_p$ ) was set to 565 V. To ensure a stable discharge, an electrical resistance was connected in series between the power supply and the discharge chamber, and set to 50  $\Omega$ . The power transferred to the plasma was adjusted by varying the time that the pulse was switched on ( $t_{ON}$ ). The pulse period used was 200  $\mu\text{s}$ . The experimental apparatus allowed to obtain both the cathodes electrical current, namely external cathode current ( $I_{EC}$ ) and central cathode current ( $I_{CC}$ ), and so the total current ( $I_T$ ), along each sintering. The temperature of the sample was selected by adjusting the on/off time of the pulsed voltage. The temperature was measured by means of a *chromel-alumel* (type K of 1.5 mm diameter) thermocouple inserted to a depth of 8 mm into the sample holder. Sintering was performed at 1423 K (1150 °C) for 60 min, with a gas flow of  $5 \times 10^{-6}$  standard  $\text{m}^3\text{s}^{-1}$ , and a gas mixture composed of 80% Ar and 20% H<sub>2</sub> at a pressure of  $1.20 \times 10^3$  Pa (9 Torr). The high pressure was adopted attempting to increase the back-diffusion effect of the sputtered atoms, decreasing the change risk of both the cathodes surface composition, and so, the contamination risk of both the cathodes, what is in accordance with (Chapman, 1980). The sintering procedure was divided into three steps:

- cleaning of the samples under a discharge at 723K (450°C) for 30 min, using  $1.33 \times 10^2$  Pa (1 Torr) pressure and the resistance adjusted to 100  $\Omega$ ;
- heating at a rate of 0.42  $\text{Ks}^{-1}$  (0.42 °C $\text{s}^{-1}$ ) and sintering at 1423K (1150°C), using  $1.20 \times 10^3$  Pa (9 Torr) pressure and resistance adjusted to 50  $\Omega$ ;
- cooling of the samples under a gas mixture flow.

For the second studied process condition, *id est* previous deposition treatment following on the hollow cathode discharge sintering, the electrodes configuration was changed to perform the previous deposition treatment. In this case, the central electrode was grounded and positively biased, working as the anode of the abnormal glow discharge, or simply as a substrate. The external cathode electrical configuration was not changed and it was maintained negatively biased. So, only it was exposed to the ion bombardment, acting as target, and so as a source of alloying

elements to the discharge, as a result of the sputtering of Fe, Cr, Ni, Mn and Si atoms. Previous deposition treatment was performed at 1123K (850 °C) sample temperature, for 60 min, with a gas flow of  $5 \times 10^{-6}$  standard  $\text{m}^3\text{s}^{-1}$  (300 sccm), and a gas mixture composed of 80% Ar and 20%  $\text{H}_2$  at a pressure of  $3.99 \times 10^2$  Pa (3 Torr). The external cathode was negatively biased at the  $730 \pm 15$  V voltage and the resistance was adjusted to 50  $\Omega$ . The heating stage of the sample up to 1123K (850 °C) was realized adjusting the resistance to 100  $\Omega$ , and maintaining the central electrode 10 min at 723K (450 °C). The  $3.99 \times 10^2$  Pa (3 Torr) pressure was chosen since higher the pressure higher is the back-diffusion effect, which results in the re-deposition of sputtered atoms on the cathode surface, decreasing the deposition rate on the substrate surface. The high temperature, 1123K (850 °C), during the deposition, was chosen attempting to reduce the risk of the oxide formation on the sample surface. The high potential (730 V) was adopted seeking to guarantee a high sputtering efficiency. As the central electrode was not exposed to the ion bombardment, the heating of the sample to the specified temperature was a result of the heat irradiated by external cathode.

So, the heating control of the sample was performed in an indirect way regulating the power transferred to the plasma, and more precisely, controlling the external cathode electrical current. Since there was no temperature control of the external cathode, an electrical current maximum limit was determined aiming at to eliminate every possibility of its melting. This limit was defined by a preliminary hollow cathode discharge sintering study as a function of the pressure, which resulted in a 650 mA maximum current of the external cathode for a  $1.20 \times 10^3$  Pa (9 Torr) pressure. This value corresponds to the highest external cathode electrical current, and thus the highest experimental severity verified in this work, to keep the sample's sintering temperature at 1423K (1150°C), as can be seen later on Table 1. Consequently, in the previous deposition treatment, the value of 650 mA external cathode current was fixed as a safety maximum limit to perform the indirect heating of the sample, keeping the cathode integrity and the stability of the discharge. After the previous deposition treatment, the deposited sample was sintered in a hollow cathode discharge configuration, in the same conditions used in the first studied process condition, returning the central electrode to be negatively biased.

Each sintering experiment was repeated three times aiming at to guarantee the results reproducibility. The samples were characterized by means of scanning electron microscopy and energy dispersive x-ray microprobe analysis, using a Philips XL-30 microscope and accessories. Characterization was carried out on the sample's lateral surface, which is the surface exposed to the glow discharge. Concentration profiles of the Cr and Ni alloying elements were obtained from cross-sectioned samples, prepared by conventional grinding and polishing techniques. Amplification of 100x resulting in a  $700 \mu\text{m} \times 900 \mu\text{m}$  scanning area was used to determine the chemical composition of sample surface. The values of it are a result of a mean and standard deviation of 9 analyses uniformly distributed along the sample lateral surface. Amplification of 1500x resulting in a  $5 \mu\text{m} \times 40 \mu\text{m}$  scanning area was used to determine the Cr and Ni concentration profiles points. Analyses were performed from  $5 \mu\text{m}$  to  $5 \mu\text{m}$ . To determine the amount of alloy elements deposited and diffused into the samples, the areas under the fitted curves for each profile were calculated by integration. Concluding, scanning electron microscopy was used too aiming at to determine qualitatively the surface morphology of the samples processed in different conditions studied.

## Results and Discussion

### Variation of the Discharge Parameters

Table 1 summarizes the variation of the macroscopic discharge parameters in a preliminary hollow cathode discharge sintering study as a function of the pressure. Pressures of  $3.99 \times 10^2$  Pa (3 Torr),  $7.98 \times 10^2$  Pa (6 Torr) and  $1.20 \times 10^3$  Pa (9 Torr) were studied. The average values shown correspond to the last 20 min at the 1423K (1150 °C) sintering temperature, along 60 min sintering time. Results indicate for the pressure range studied that higher the pressure higher is the total current. Despite the central cathode current ( $I_{CC}$ ) increasing slightly, the same is not observed since the external cathode current ( $I_{EC}$ ) strongly increase. This is probably related to the plasma species energy. It is know the mean free path vary inversely with pressure (Chapman, 1980). As a result, the ions and electrons energy decrease strongly for the highest pressure, being necessary to increase the power transferred to the plasma, what was effectively verified by adjusting for a higher value the time that the pulse was switched on ( $t_{ON}$ ). Besides, the external cathode area exposed to the plasma is much higher than the central cathode area what is direct related to this result.

**Table 1. Variation of the macroscopic discharge parameters as a function of the pressure, in the hollow cathode discharge sintering experiments.**

Pressure (Torr)	T (°C)	$t_{ON}$ ( $\mu\text{s}$ )	$I_{CC}$ (mA)	$I_{EC}$ (mA)	$I_T$ (mA)
3	$1153 \pm 1,0$	$41 \pm 1,0$	$159 \pm 1,0$	$299 \pm 3,5$	$458 \pm 4,5$
6	$1151 \pm 2,0$	$37 \pm 0,5$	$161 \pm 1,5$	$393 \pm 2,5$	$554 \pm 3,5$
9	$1150 \pm 3,0$	$59 \pm 1,0$	$184 \pm 2,0$	$586 \pm 5,5$	$770 \pm 6,0$

Figure 2 depicts the evolution of the discharge parameters as a function of time, in a hollow cathode discharge sintering experiment performed at  $1.20 \times 10^3$  Pa (9 Torr) pressure. It emphasizes the heating from 723K (450°C) to 1423K (1150 °C) and sintering stages. The discharge worked in stable way in abnormal glow regime along all process. The maximum current were verified in the start of sintering step, attaining 650 mA. In this condition, according to the results from Table 1, the total current average of the last 20 min was 770 mA. As previously seen, the electrical current of the external cathode was defined as the control parameter for the previous deposition treatment, and this value of 650 mA was fixed as a safety limit to perform the indirect heating of the sample.

Figure 3 presents the evolution of the discharge parameters as a function of time, for a complete experiment comprising a previous deposition treatment following on the hollow cathode discharge sintering. In deposition treatment the maximum current measured at the external cathode was 386 mA and average value related to the last 20 min at the deposition temperature, 1123K (850 °C), was 325 mA, exactly half of the 650 mA value. As expected, there was no current at the central electrode and his heating was performed as a result of the radiation emitted from the external cathode surface, which heated the anode parts, and so the central electrode. Sintering treatment started as the central electrode reached 343K (70 °C) temperature, after cooling under gas mixture flow.

## Characterization of the Processed Samples

### Hollow Cathode Discharge Sintering Experiment

Figures 4 and 5 presents the results obtained in a hollow cathode discharge sintering experiment performed at  $1.20 \times 10^3$  Pa (9 Torr) pressure.

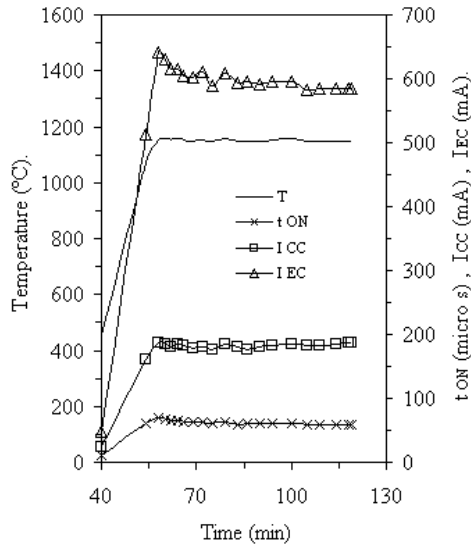


Figure 2. Evolution of the discharge parameters as a function of time.

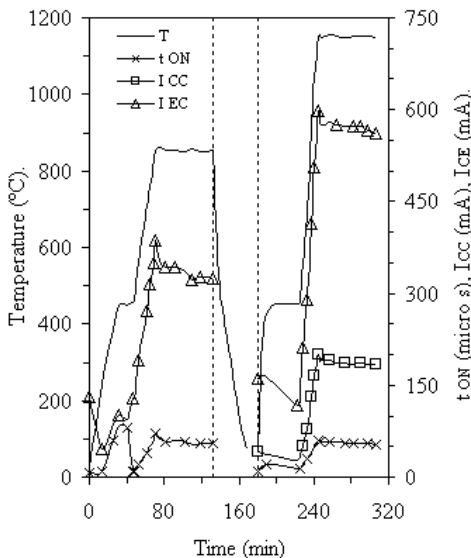


Figure 3. Evolution of the discharge parameters as a function of time, for a complete experiment comprising a previous deposition treatment following on the hollow cathode discharge sintering.

The surfaces of the samples were characterized in terms of their chemical composition and morphology. Figure 4 shows Cr and Ni concentration profiles. The concentration of atoms on the surface was around 2.8% and 1.7% for Cr and Ni, respectively, which were attributed to the sputtering occurring in the hollow cathode discharge. Furthermore, with 60 min sintering time, the depth of the layer containing alloying elements increased to more than 20  $\mu\text{m}$  for Cr and 17  $\mu\text{m}$  for Ni, as expected for diffusion mechanisms. The data shown in Fig. 4 were mathematically treated to quantify the actual amounts of Cr and Ni deposited on and diffused into the

samples. The equations of the fitted curves for the Cr and Ni profiles, Eq. (1) and Eq. (2) respectively, were:

$$y(\text{Cr}) = 0.0018 x^2 - 0.1557 x + 2.6989 \quad (R^2 = 0.9955) \quad (1)$$

and

$$y(\text{Ni}) = 0.0031 x^2 - 0.1466 x + 1.6615 \quad (R^2 = 0.9937) \quad (2)$$

An integration of the Eq. (1) and Eq. (2) using the limits defined in the graph yielded the respective calculated areas expressed in ( $\mu\text{m} \times \text{at.}\%$ ). The mathematical treatment was the same used in (Brunatto et al., 2005). The calculated values were 28 ( $\mu\text{m} \times \text{at.}\%$  Cr) and 12 ( $\mu\text{m} \times \text{at.}\%$  Ni), respectively. These values express the effective amounts of Cr and Ni that were diffused into the sample.

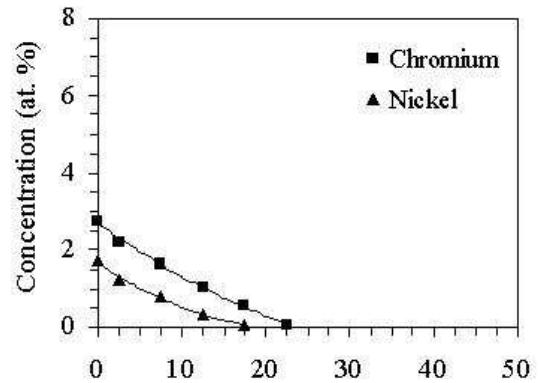


Figure 4. Cr and Ni concentration profiles for a sample processed in a hollow cathode discharge sintering at  $1.20 \times 10^3$  Pa (9 Torr) pressure.

Figure 5 confronts, in a same region, the surface morphology of the pressed (Fig. 5a) and as sintered (Fig.5b) sample. The ion bombardment produced a slight modification of the surface morphology. It is to be noted there is no evidence of the surface densification as a result of the sputtering mechanism, since the pores initially presented on the pressed (green) sample's surface maintain practically unaltered their sizes and shapes after sintering. The mass loss measurement of the sample sintered at  $1.20 \times 10^3$  Pa (9 Torr) pressure taken to evaluate the sputtering effect on the central cathode was 6.6 mg (0.13%), confirming the slight sputtering that occurred in the central cathode. It should be noted that the alteration of the surface morphology of the sample was congruent with the mass loss and it is in accordance with the results presented in a previous work (Brunatto, 2005), since the mass loss of the sample sintered at  $3.99 \times 10^3$  Pa (3 Torr) pressure during 60 min, was 23.2 mg (0.46%). So, the slight modification of the surface morphology evidenced on Fig. 5 is a result of the use of a high pressure, which tends to increase the back-diffusion effect of the sputtered atoms, decreasing the risk of the surface morphology modification. It also explains the results presented on Fig. 4, *id est* the low concentration of Cr and Ni atoms verified on the surface exposed to the plasma.

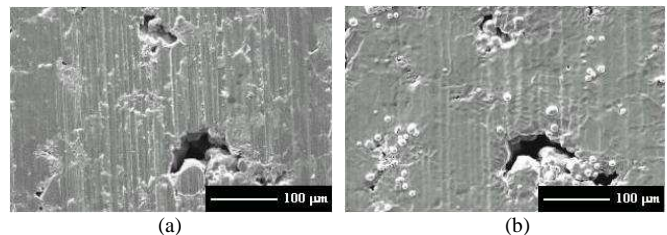


Figure 5. Surface morphology in a same region of the: a) pressed (green) sample; and b) as sintered (sample processed in a hollow cathode discharge sintering at  $1.20 \times 10^3$  Pa -9 Torr- pressure).

### Previous Deposition Experiment

Figure 6 depicts the results obtained in pressed samples submitted to a previous deposition treatment. The surface of the sample was characterized in terms of their chemical composition and morphology. As can be seen (Fig. 6a), a significant deposition of alloying elements was obtained. The concentration of atoms on the surface was around 15.5% and 16.2%, for Cr and Ni, respectively, which were attributed to the intense sputtering occurring in the inner surface of the external cathode. The occurrence of oxygen atoms on the deposit layer is probably due to the smaller temperature of the central electrode than the external cathode. It is known the stability of oxide phases tends to increase as the temperature diminishes. Besides, impurities like oxygen atoms tend to condense next to the colder surfaces. As the central electrode is electrically grounded and positively biased there is no bombardment of positive ions in it, which facilitates the permanence of impurities due to absence of sputtering. It is important emphasizing oxygen occurs on the original iron particle surfaces of the pressed (green) samples, in the iron oxide way. So, the pressed sample becomes a powerful oxygen source. As the chromium oxide is much more thermodynamically stable than the iron oxide, and there is a significant thermal activation on the central electrode (1123K -850 °C-) combined to the presence of hydrogen at the discharge, the occurrence of oxygen on the deposit layer could be expected. Figure 6(b) presents the morphology of the deposit layer.

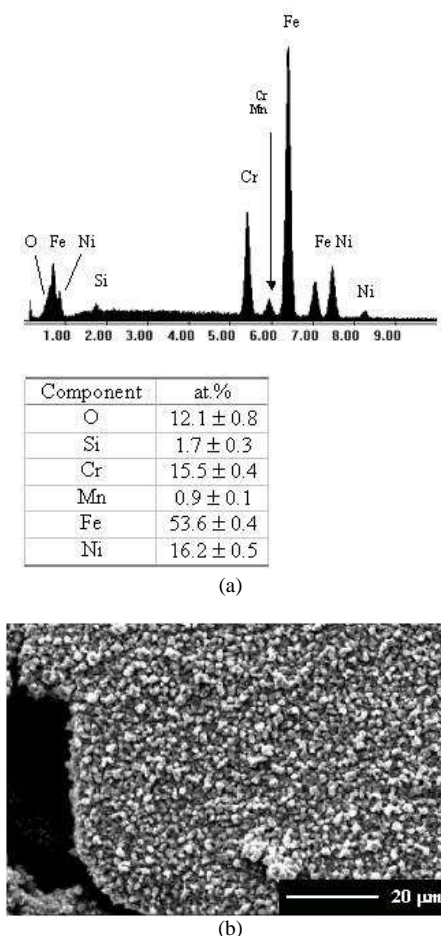


Figure 6. Surface chemical composition (a) and morphology (b) for a pressed samples submitted to a previous deposition treatment.

The product of the deposition treatment is clearly formed by micrometric and nanometric particles as a result of the atoms clustering. This result is in accordance with (Romanowsky and Wronikowski, 1992) that reported the production of TiN layer in reactive pulse plasma as a result of deposition of clusters plus ions formed at the plasma and their coagulation or sintering at the substrate surface, comprising a typical morphology of powder particle.

### Previous Deposition Treatment Following on the Hollow Cathode Discharge Sintering Experiment

Figures 7, 8 and 9 present the results obtained in previous deposition treatment following on the hollow cathode discharge sintering experiment. The surface of the sample was characterized in terms of their chemical composition and morphology. Figure 7 shows Cr and Ni concentration profiles. The concentration of atoms on the surface was around  $6.5 \pm 0.3\%$  and  $6.9 \pm 0.3\%$  for Cr and Ni, respectively. Furthermore, after the sintering stage, the depth of the layer containing alloying elements increased to more than  $45 \mu\text{m}$  for Cr and  $40 \mu\text{m}$  for Ni, as expected for diffusion mechanisms. The data shown in Fig. 7 were also mathematically treated to quantify the actual amounts of Cr and Ni deposited on and diffused into the samples. The equations of the fitted curves for the Cr and Ni profiles, Eq. (3) and Eq. (4) respectively, were:

$$y(\text{Cr}) = 0.0016 x^2 - 0.2128 x + 6.6571 \quad (R^2 = 0.985) \quad (3)$$

and

$$y(\text{Ni}) = 0.004 x^2 - 0.3286 x + 7.0576 \quad (R^2 = 0.986) \quad (4)$$

An integration of the Eq. (3) and Eq. (4) using the limits defined in the graph yielded the calculated areas of  $133 (\mu\text{m} \times \text{at.}\% \text{Cr})$  and  $105 (\mu\text{m} \times \text{at.}\% \text{Ni})$ , respectively. As expected, these results clearly indicate much higher effective amounts of Cr and Ni diffused into the sample submitted to a deposition and sintering experiment than into the sample only sintered (Fig. 4).

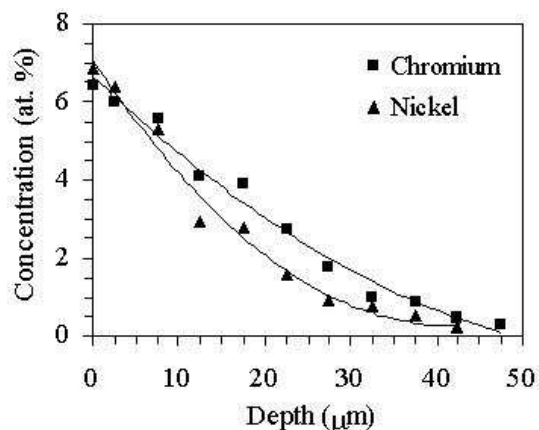


Figure 7. Cr and Ni concentration profiles for a sample submitted to a previous deposition treatment following on the hollow cathode discharge sintering experiment.

Figure 8 shows two images of a polished iron sample cross section. It can be noted next to the lateral surface of the sample (Fig. 8a) a disperse net of second phase particles indicated by arrows. The presence of them is better characterized in Fig. 8(b), with a higher magnitude. The accurate chemical analysis of these particles



indicated the occurrence of Cr and Fe compound oxides precipitated along the diffusion layer (Fig. 8c). These results are in agreement with that of the Fig. 6, as previously discussed, being explained by the high affinity between Cr and oxygen.

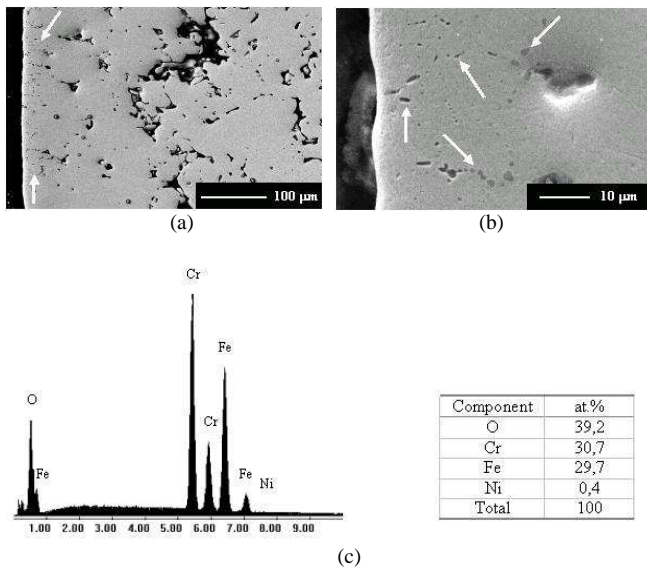


Figure 8 - Sample submitted to a previous deposition treatment following on the hollow cathode discharge sintering experiment: a) polished cross section image next to the lateral surface of the sample; b) the same with a higher magnitude; and c) accurate chemical analysis of the second phase.

Figure 9 compares in a same region, the surface morphology of the pressed (Fig. 9a) and as deposited and sintered sample (Fig. 9b). Note in Fig. 9(b), the deposit layer obtained in the previous deposition treatment (Fig. 6b) was eliminated as a result of the ion bombardment at the hollow cathode sintering stage. Besides, it is possible the ion bombardment tends to activate the surface diffusion mechanisms. This assumption is in agreement with the higher diffusion depth verified in Fig. 7, which is also a consequence of the higher Cr and Ni concentration gradients present on the deposited surface. Finally, a similar result evidenced for the hollow cathode discharge sintered sample (Fig. 5) was obtained for the deposited and sintered sample (Fig. 9), *id. est* a slight modification of the surface morphology, since the same sintering parameters were used in both the studied conditions. It must be emphasized in the results presented at Fig.9 there is again no evidence of the surface densification as a result of the sputtering mechanism, since the pores initially presented on the pressed (green) sample's surface maintain practically unaltered their sizes and shapes after sintering. This explains why no attention was spent to determine the densification level of the surfaces exposed to the plasma, and to confront the bulk densification level for the samples 7.0 g cm<sup>-3</sup> density processed in this work.

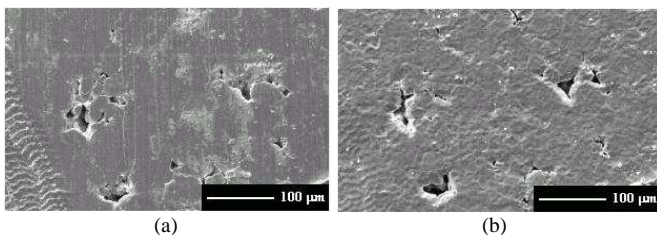


Figure 9. The surface morphology in a same region of the: a) pressed; and b) as deposited and sintered sample.

## Conclusion

The use of a deposition treatment performed previously to the hollow cathode discharge sintering allow optimizing the amount of alloying elements deposited and diffused into the iron sample's surface, granting this alternative procedure potentially applicable to change the chemical composition of the surface of sintered components. Our results demonstrate the viability of sintering samples consisted initially of pure iron and promoting Cr and Ni enrichment on their surfaces, for 6.5 at.% and 6.9 at.% values, respectively. The surface finishing of iron samples presented slightly changed after sintering, qualitatively evidenced by a more roughness texture than that in the as pressed (green) condition, as a result of the sputtering. At least to the studied conditions here, there is no evidence indicating the deposition and sintering process in hollow cathode discharge is adequate to obtain surface densification of iron samples. Otherwise, the intense ion bombardment may produce a significant modification of the sample surface morphology, and it may be a great allied in a densification of porous surface. At this moment, further studies are being carried out so as to investigate it.

## References

- Batista, V.J., Mafra, M., Muzart, J.L.R., Klein, A.N., 1998, "Sintering Iron Using an Abnormal Glow Discharge", *The International Journal of Powder Metallurgy*, v.34, n.8, pp.55-62.
- Benda M., Vlcek J., Cibulka V., Musil J., 1997, "Plasma Nitriding Combined With a Hollow Cathode Discharge Sputtering at High Pressures". *J. Vac. Sci. Technol. A*, v.15, n.5, pp. 2636-2643.
- Bengisu, M., Inal, O.T., 1994, "Sintering of MgO and MgO-TiC Ceramics by Plasma, Microwave and Conventional Heating". *Journal of Materials Science*, v.29, pp. 5475-5480.
- Brunatto, S. F., Kühn, I., Muzart, J. L. R., 2001, "Influence of the Radial Spacing Between Cathodes on the Surface Composition of Iron Samples Sintered by Hollow Cathode Discharge". *Materials Research*, v. 4, n.4, pp.245-250.
- Brunatto, S.F., Khün, I., Muzart, J.L.R., 2005, "Surface Modification of iron Sintered in Hollow cathode Discharge Using an External Stainless Steel Cathode". *J. Phys. D: Appl. Phys.*, v.38, pp.2198-2203.
- Chapman, B., 1980, "Glow Discharge Processes: Sputtering and Plasma Etching", John Wiley & Sons, New York, USA, p. 100.
- Hashiguchi, S., Hasikuni, M., 1987, "Theory of the Hollow Cathode Glow Discharge". *Japanese Journal of Applied Physics*, v.26, n.2, pp. 271-280.
- Jones, G., et al., 1994, "Plasma Activated Sintering (PAS) of Tungsten Powders". *Materials and Manufacturing Processes*, V. 9, n. 6, pp. 1105-1114.
- Koch, H. et al., 1991, "Hollow Cathode Discharge Sputtering Device for Uniform Large Area Thin Film Deposition". *J. Vac. Sci. Technol. A*, v.9, n.4, pp. 2374-2377.
- Kolobov, V. I., Tsendin, L. D., 1995, "Analytical Model of the Hollow Cathode Effect". *Plasma Sources Sci. Technol.*, v.4, pp. 551-560.
- Muzart, J.L.R., Batista, V.J., Franco, C.V., Klein, A.N., 1997, "Plasma Sintering of AISI 316L Stainless Steel: The influence of the Processing Cycle on the Sample Density". *Proceedings of Advances in Powder Metallurgy & Particulate Materials - MPIF*, Part 3, pp.77-84.
- Onagawa, J. et al., 1996, "Corrosion Resistance of Titanium-Platinum Alloy Prepared by Spark Plasma Sintering". *Materials Transactions, JIM*, v.37, n.11, pp. 1699-1703.
- Romanowsky, Z., Wronikowski, M., 1992, "Specific Sintering by Temperature Impulses as a mechanism of Formation of a TiN Layer in the Reactive Pulse Plasma". *Journal of Materials Science*, v. 27, pp.2619-2622.
- Schaefer, G. et al., 1984, "Pulsed Hollow Cathode Discharge with Nanosecond Risetime". *IEEE Transactions on Plasma Science*, v.PS-12, n.4.
- Su, H., Johnson, D. L., 1996, "Sintering of Alumina in Microwave-Induced Oxygen Plasma". *J. Am. Ceram. Soc.*, v.79, n.12, pp. 3199-3210.

Tandian, N. P., Pfender, E., 1997, "*Heat Transfer in RF Plasma Sintering: Modeling and Experiments*". Plasma Chemistry and Plasma Processing, v.17, n.3, pp. 353-370.

Terakado K., Urao R., Ohmori M., 1996, "*Simultaneous Plasma Treatment for Carburising and Carbonitriding using Hollow Cathode*

*Discharge*". Metallurgical and Materials Transactions A, v.27A, pp.401-405.

Timanyuk V. A., Tkachenko V. M., 1989, "*Study of a Glow Discharge in an Annular Cathode Cavity*". Sov. Phys. Tech. Phys., v.34, n.7, pp.832-834. v. Engel, A., 1994, "*Ionized Gases*". 2<sup>nd</sup> ed., American Institute of Physics, New York, USA, p.325.